Microscopic mechanism of charged-particle radioactivity and generalization of the Geiger-Nuttall law

C. Qi,[1,2] F.R. Xu,[1,3] R.J. Liotta,[2] R. Wyss,[2]

M.Y. Zhang,[1] C. Asawatangtrakuldee,[1] and D. Hu[1]

[1]*School of Physics, and State Key Laboratory of Nuclear Physics and Technology, Peking University, Beijing 100871, China*

[2]*KTH (Royal Institute of Technology), Alba Nova University Center, SE-10691 Stockholm, Sweden*

[3]*Center for Theoretical Nuclear Physics, National Laboratory for Heavy Ion Physics, Lanzhou 730000, China*

(Dated: September 24, 2009)

Abstract

A linear relation for charged-particle emissions is presented starting from the microscopic mechanism of the radioactive decay. It relates the logarithms of the decay half-lives with two variables, called χ' and ρ', which depend upon the Q-values of the outgoing clusters as well as the masses and charges of the nuclei involved in the decay. This relation explains well all known cluster decays. It is found to be a generalization of the Geiger-Nuttall law in α radioactivity and therefore we call it the universal decay law. Predictions on the most likely emissions of various clusters are presented by applying the law over the whole nuclear chart. It is seen that the decays of heavier clusters with non-equal proton and neutron numbers are mostly located in the trans-lead region. The emissions of clusters with equal protons and neutrons, like ^{12}C and ^{16}O, are possible in some neutron-deficient nuclei with $Z \geq 54$.

PACS numbers: 21.10.Tg, 23.60.+e, 23.70.+j, 27.60.+j, 27.90.+b

I. INTRODUCTION

Charged-particle emissions are among the most important decay modes of atomic nuclei. Almost all observed proton-rich exotic nuclei starting from $A \sim 150$ are α radioactive [1]. A substantial number of proton decays have been observed in proton-drip-line nuclei around the rare earth region [2]. The spontaneous emission of charged fragments heavier than the α particle (cluster decay) was predicted in Ref. [3] and later established experimentally in trans-lead mother nuclei decaying into daughters around the doubly magic nucleus ^{208}Pb [4, 5, 6, 7]. Even a second island of cluster radioactivity was predicted in trans-tin nuclei decaying into daughters close to the doubly magic nucleus ^{100}Sn [8].

A number of theoretical models were proposed to describe the charged-particle decay process [9, 10, 11, 12, 13, 14, 15, 16, 17, 18, 19] (see also Refs. [20, 21, 22, 23, 24, 25] for very recent calculations). In general the decay process, ranging from proton to heavier cluster radioactive decays, can be described by a two-step mechanism [26]. The first step refers to the formation of the particle and its motion on the daughter nuclear surface. In the second step the cluster, with the formation amplitude and corresponding wave function thus determined, is assumed to penetrate through the centrifugal and Coulomb barriers [27, 28, 29, 30]. This second step is well understood since the pioneering work of Gamow [27]. In macroscopic models, cluster decay is treated as the quantum tunneling process of an already preformed particle [12, 13, 21, 22, 23, 24, 25], where features like the probability that the cluster is formed on the nuclear surface are ignored. In these models the clusterization process is included in an effective fashion by introducing quantities adjusted to reproduce as many measured half-lives as possible. Such semiclassical models are being successfully applied even at present, although in some cases microscopical ingredients are also included [12]. In microscopic theories the formation amplitude is evaluated starting from the single-particle degrees of freedom of the neutrons and protons that eventually become the cluster. This is generally a formidable task which requires advanced computing facilities as well as suitable theoretical schemes to describe the clusterization process [15, 16, 17, 18].

On the other hand, this variety of theoretical models may serve as a guide to our searching of semiclassical relations in the radioactive decay. The first striking correlation in α decay systematics was noted by Geiger and Nuttall [31]. This relates the decay half-lives $T_{1/2}$ and

decay energies Q_α as,

$$\log T_{1/2} = aQ_\alpha^{-1/2} + b, \tag{1}$$

where a and b are constants. Nowadays it is understood that the Q-value dependence in Eq. (1) is a manifestation of the quantum penetration of the α-cluster through the Coulomb barrier (see, for example, Ref. [32]). But this equation ignores the probability that the α-particle is formed on the nuclear surface starting from its four constituent nucleons moving inside the mother nucleus. The linear relation (1) has been found to hold well for the ground-state to ground-state decays of even-even nuclei in the same major shell with fixed proton number. However, the Geiger-Nuttall law in the form of Eq. (1) has limited prediction power since the coefficients a and b change for the decays of different isotopic series [33]. Intensive works have been done trying to generalize the Geiger-Nuttall law for a universal description of all observed α decay events [33, 34, 35, 36, 37, 38]. For example, in the work of Viola and Seaborg [33], the a and b coefficients of Eq. (1) are assumed to be linearly dependent upon the charge number of the daughter nucleus. But the physical origin of this dependence is not clear. Empirical linear relations were also found in the cases of proton decays [39, 40, 41], heavier cluster decays [29, 42, 43, 44] and both α and heavier cluster decays [45, 46, 47]. Reviews on existing empirical relations can be found in Refs. [37, 46] and thus will not be detailed here. In particular, some recent searches of correlations in radioactive decays start from the macroscopic description of the decay process with a concentration on the Coulomb barrier penetrability [32, 34, 37, 45], which are physically more sound than mere empirical relations. But in these macroscopic approaches one has to assume an effective interaction between the cluster and the core [32, 34]. Besides, an effective spectroscopic factor (formation amplitude) has to be introduced [37] which, however, is model-dependent and sensitive to details of the effective interaction.

In a recent Letter [48], we have introduced a linear universal decay law (UDL) starting from the microscopic mechanism of the charged-particle emission. Our aim was to find a general framework valid for all clusters, which may be used in the future as a gauge to probe effective formulas. This is an interesting subject in itself, but perhaps even more important is that it may help in the ongoing searching of new cluster decay modes from superheavy nuclei [29]. The UDL relates the half-lives of monopole radioactive decays with the Q-values of the outgoing particles as well as the masses and charges of the nuclei involved in the decay, reflecting quite well the systematical trend of experimental data. In this paper we

will complete the brief presentation given in Ref. [48] with details of the construction of the formula and approximations leading to it. Besides, we present the predictions of the UDL on the most likely emissions of various clusters.

In Section II is the Formalism. In Section III systematics of experimental α and cluster decay half-lives are analyzed and compared with the corresponding calculations. In Section IV possible observations of new cluster decays are suggested. A Summary and the Conclusions are in Section V.

II. FORMALISM

In a classic paper [26], Thomas derived the expression of the cluster decay width by evaluating the residues of the corresponding S-matrix in the framework of the R-matrix theory [49]. The decay half-life thus obtained has the form,

$$T_{1/2} = \frac{\hbar \ln 2}{\Gamma_c} = \frac{\ln 2}{\nu} \left| \frac{H_l^+(\chi,\rho)}{RF_c(R)} \right|^2 , \tag{2}$$

where Γ_c is the decay width, ν the outgoing velocity of the charged particle carrying an angular momentum l. R is the distance between the corresponding centers of mass of the cluster and daughter nucleus, which should be large enough that the nuclear interaction is negligible. H_l^+ is the Coulomb-Hankel function and its arguments are standard, i.e., $\rho = \mu\nu R/\hbar$ and the Coulomb parameter is $\chi = 2Z_cZ_de^2/\hbar\nu$ with μ being the reduced mass of the cluster-daughter system and Z_c and Z_d the charge numbers of the cluster and daughter nucleus, respectively. Eq. (2) contains the two-step mechanism mentioned above. The quantity $F_c(R)$ is the formation amplitude of the decaying particle at distance R, which is usually evaluated as the overlap between the mother wave function and the antisymmetrized tensor product of the daughter and cluster wave functions. The penetrability is proportional to $|H_l^+(\chi,\rho)|^{-2}$. This equation is the basis of all microscopical calculations of radioactive decay processes [16, 39]. It is valid for all clusters and for spherical as well as deformed cases. The ratio $N_l = RF_c(R)/H_l^+(R)$, and therefore the half-life itself, is independent of the radius R [16]. In Ref. [50] it is shown that the expression of Eq. (2) coincide with the quantum-mechanical interpretation of the half-life as the outgoing flux per unit of time.

In what follows we will apply the exact expression of Eq. (2). Our aim is to find a few quantities that determine the half-life. Expanding in these quantities we hope to be able to

find, at the lowest order of perturbation, an expression of the half-life which is as simple as the Geiger-Nuttall law but valid in general, i.e., for all isotopic series as well as all type of clusters. This is possible since Eq. (2) itself is valid in general. The number of variables that we have to look for should be small for cases of interest, i.e., for the decay of medium and heavier nuclei. In fact most interesting is the predicting power with respect to superheavy nuclei, which are at the center of attention of present experimental activities. With this in mind we notice that the Coulomb-Hankel function can be well approximated by an analytic formula, which for the $l = 0$ channel reads [51],

$$H_0^+(\chi,\rho) \approx (\cot\beta)^{1/2} \exp\left[\chi(\beta - \sin\beta\cos\beta)\right], \tag{3}$$

where the cluster Q-value is $Q_c = \mu\nu^2/2$ and

$$\cos^2\beta = \frac{\rho}{\chi} = \frac{Q_c R}{e^2 Z_c Z_d}. \tag{4}$$

One sees that $\cos^2\beta$ would be a small quantity if $Z_c Z_d$ is large. In this case one can expand the last term in a power series of $\cos\beta$ (with $\beta = \arccos(\cos\beta)$) as,

$$\beta - \sin\beta\cos\beta = \frac{\pi}{2} - 2\cos\beta + \frac{\cos^3\beta}{3} + \frac{\cos^5\beta}{20} + \cdots, \tag{5}$$

and for medium and heavier nuclei (the heavier the better) terms beyond the third order can be neglected. One obtains,

$$\log\frac{|H_0^+(\chi,\rho)|^2}{\cot\beta} \approx \frac{2\chi}{\ln 10}\left[\frac{\pi}{2} - 2\left(\frac{\rho}{\chi}\right)^{1/2} + \frac{1}{3}\left(\frac{\rho}{\chi}\right)^{3/2}\right], \tag{6}$$

and therefore,

$$\begin{aligned}\log T_{1/2} \;\approx\; & \frac{2\chi}{\ln 10}\left[\frac{\pi}{2} - 2\left(\frac{\rho}{\chi}\right)^{1/2} + \frac{1}{3}\left(\frac{\rho}{\chi}\right)^{3/2}\right] \\ & + \log\left(\frac{\cot\beta\ln 2}{\nu R^2 |F_c(R)|^2}\right),\end{aligned} \tag{7}$$

which is dominated by the first two terms. For the radius R in above equation, one can take the standard value of $R = R_0(A_d^{1/3} + A_c^{1/3})$ with $R_0 \sim 1.2$ fm [39, 48]. Defining the factors χ' and ρ' as,

$$\begin{aligned}\chi' &= \frac{\hbar}{e^2\sqrt{2m}}\chi = Z_c Z_d\sqrt{\frac{A}{Q_c}}, \\ \rho' &= \frac{\hbar}{\sqrt{2mR_0e^2}}\left(\rho\chi\right)^{1/2} \\ &= \sqrt{AZ_cZ_d(A_d^{1/3} + A_c^{1/3})},\end{aligned} \tag{8}$$

where $A = A_d A_c/(A_d + A_c) = \mu/m$ and m is the nucleon mass (within the errors of our treatment we take $mc^2 \approx 938.9$ MeV and $\hbar c = 197.3$ MeV fm), one gets

$$\begin{aligned} \log T_{1/2} &= \frac{\sqrt{2M}e^2\pi}{\hbar \ln 10}\chi' - \frac{4e\sqrt{2MR_0}}{\hbar \ln 10}\rho' \\ &\quad + \log\left(\frac{\cot\beta \ln 2}{\nu R^2 |F_c(R)|^2}\right) + o(3), \\ &= a\chi' + b\rho' - 2\log|F_c(R)| + c, \end{aligned} \tag{9}$$

where a and b are constants and $o(3)$ corresponds to the remaining small terms in the Coulomb penetration. The terms $o(3)$ and $\log\cot\beta/(\nu R^2)$ change rather smoothly for the decay cases of interest and may be safely approximated as a constant c.

A straightforward conclusion from Eq. (9) is that $\log T_{1/2}$ depends linearly upon χ' and ρ'. Still the strong dependence of the formation probability upon the cluster size has to be taken into account by Eq. (9). This seems to be a difficult task, since the formation probability is strongly dependent upon the nuclear structure of the nuclei to be analyzed. In other words, if such a simple linear relation is correct one has to be able to demonstrate that the formation amplitude depends only linearly upon χ', ρ' or an additional variable. We found that this is indeed the case by exploiting the property that for a given cluster $N_0 \equiv RF_c(R)/H_0^+(\chi,\rho)$ does not depend upon R. Using the approximations leading to Eq. (9) one readily obtains the relation,

$$\log\left|\frac{R'F_c(R')}{RF_c(R)}\right|^{-2} \approx \frac{4e\sqrt{2M}}{\hbar \ln 10}\left(\sqrt{R'_0} - \sqrt{R_0}\right)\rho', \tag{10}$$

where $R' = R'_0(A_d^{1/3} + A_c^{1/3})$ is a value of the radius that differs from R. The above equation can also be written as,

$$\log|RF_c(R)| \approx \log|R'F_c(R')| + \frac{2e\sqrt{2M}}{\hbar \ln 10}\left(\sqrt{R'_0} - \sqrt{R_0}\right)\rho'. \tag{11}$$

Since for a given cluster any nuclear structure would be carried by the terms $RF_c(R)$ and $R'F_c(R')$ in exactly the same fashion, Eq. (11) implies that the formation amplitude is indeed linearly dependent upon ρ'. Therefore one can write [48],

$$\log T_{1/2} = a\chi' + b\rho' + c. \tag{12}$$

The coefficients b and c in this relation are different from that of Eq. (9) since the terms $b\rho' + c$ have to include the effects that induce the clusterization in the mother nucleus.

This relation holds for the monopole radioactive decays of all clusters and we called it the UDL [48]. The relation can be easily generalized to include the $l \neq 0$ decay cases by taking the effects of the centrifugal potential on the barrier penetrability into account [51].

It can be easily recognized that the UDL includes the Geiger-Nuttall law as a special case since ρ' remains constant for a given α-decay chain and $\chi' \propto Q_c^{-1/2}$. Besides, one basic assumption behind the relation (12) is that one can define a proper radius R' that leading to a stable formation amplitude $F_c(R')$ for all cluster radioactivities. In the next Section we will probe these conclusions, and the approximations leading to them.

III. SYSTEMATICS OF EXPERIMENTAL DATA

In this Section we will analyze ground-state to ground-state radioactive decays of even-even nuclei. We take all α decay events from emitters with $78 \leq Z \leq 108$ for which experimental data are available to us. We take the data from the latest compilations of Refs. [1, 52] and the lists of Refs. [22, 53]. For the decay of heavier clusters we have selected 11 measured events ranging from ^{14}C to ^{34}Si [7]. The branching ratios of the cluster decays relative to the corresponding α decay are in the range of 10^{-9} to 10^{-16}. The partial half-lives of observed cluster decays are between 10^{11}s and 10^{28}s.

A. Experimental constraint on the formation amplitude

The formation amplitude $F_c(R)$ reflects the nuclear structure effect on the cluster decay process. According to Eq. (2) the formation amplitude $F_c(R)$ can be extracted from experimental data as,

$$\log|RF_c(R)| = -\frac{1}{2}\log T_{1/2}^{\text{Expt.}} + \frac{1}{2}\log\left[\frac{\ln 2}{\nu}|H_0^+(\chi,\rho)|^2\right]. \tag{13}$$

By using $R_0 = 1.2$ fm we evaluated the function $\log|RF_c(R)|$ corresponding to α clusters to obtain the results plotted in Fig. 1. One sees that as a function of the charge number of the emitters the formation probabilities are located in the range $\log|RF_c(R)| = -1.5 \sim -0.75$ fm$^{-1/2}$ with about half of the data below -1.0 fm$^{-1/2}$. The formation amplitude is therefore in the range $F_c(R) = (0.03 \sim 0.18)/R$ (where R is in fm and $F_c(R)$ in fm$^{-3/2}$). One thus confirms that for a given cluster the formation amplitude is constant within an

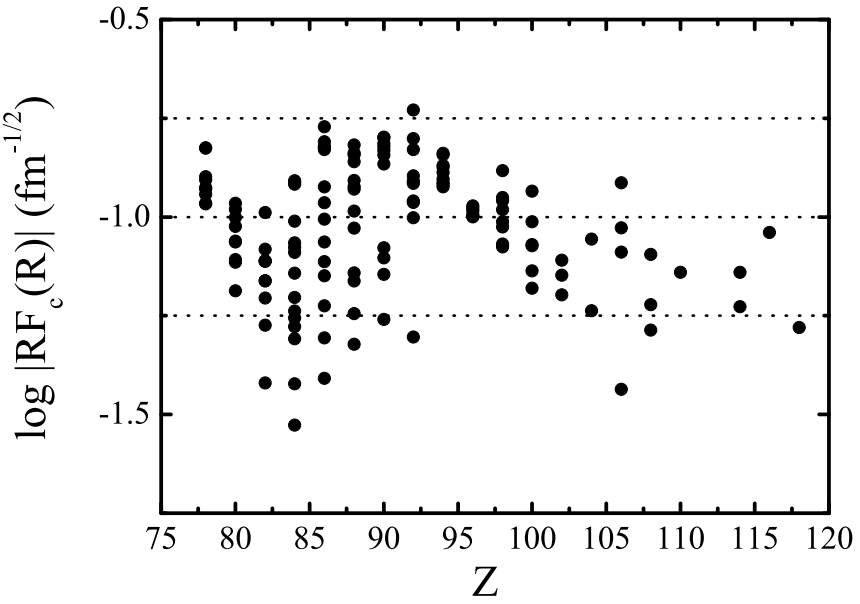

FIG. 1: The α decay formation amplitudes $\log|RF_c(R)|$ as a function of the charge number of the mother nucleus Z.

order of magnitude. The stability of the α decay formation amplitude indicates that the linear relation described by Eq. (12) is not as unexpected as one might have assumed.

It is seen from Fig. 1 that in a few cases the formation amplitudes become small, i.e., with the $\log|RF_c(R)| < -1.4$ fm$^{-1/2}$. These correspond to the α decays of nuclei ^{194}Pb, ^{208,210}Po, ^{212}Rn and ^{266}Sg (note that the error in the experimental half-life of this nucleus is still large [1, 54]). The α formation amplitudes may have been significantly reduced in the former four nuclei which are approaching the $Z = 82$ and/or $N = 126$ shell closures.

Following the same procedure as above we evaluated $\log|RF_c(R)|$ for observed heavy clusters, as seen in Fig. 2. One sees that now $\log|RF_c(R)|$ is in the range -9 to -3, i.e., $F_c(R) = (10^{-9} - 10^{-3})/R$ fm$^{-3/2}$. Given the variety of clusters (from ^{14}C to ^{34}Si) involved in the Figure this wide range of 6 orders of magnitude is also expected.

We are now in a position to probe the validity of the linear relation between the logarithm of the formation probability as a function of ρ' as implied by Eq. (11). As seen in Fig. 3 that relation holds rather well. The majority of available experimental data corresponds to α-decay. Since the formation amplitude of a given type of cluster is rather constant one sees in the Figure an accumulation of black points around $\log|RF(R)| \approx -1.2$ fm$^{-1/2}$. This

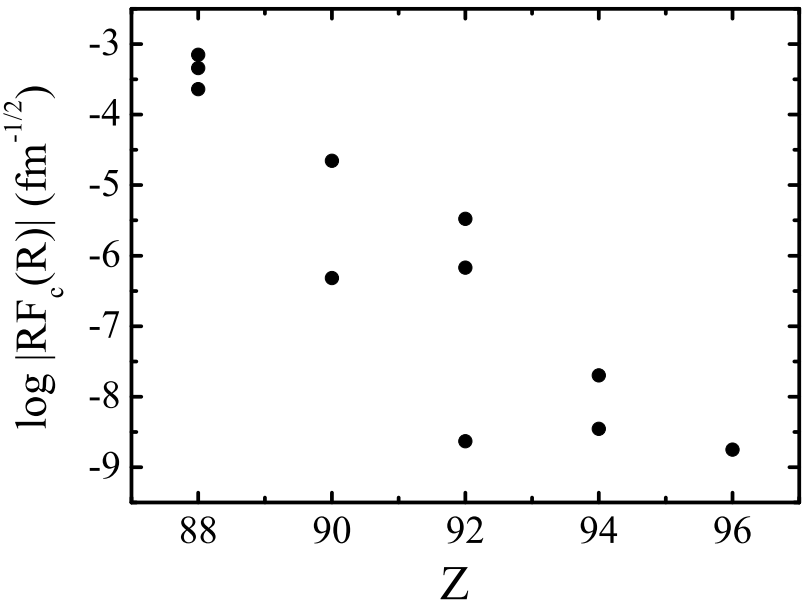

FIG. 2: Same as Fig. 1 but for those of heavier cluster decays.

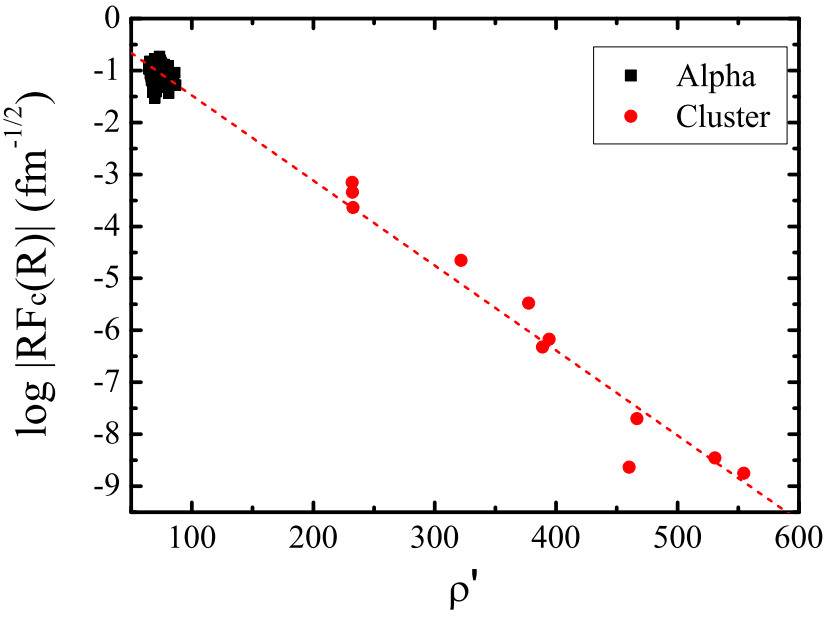

FIG. 3: (Color online) The formation amplitudes $\log|RF_c(R)|$ for both α and cluster decays as a function of ρ'.

corresponds to α-decay events. For the other clusters the formation probabilities decrease, as expected. The important point that one can make from the Figure is that the predicted linear trend is confirmed. The linear trend of experimental data ensures that one can find an radius R' where $F_c(R')$ remain constant for all radioactivities. The R' value can be determined through a fitting procedure.

There is a deviation to this trend at $\rho' \approx 460$ which corresponds to the decay of $^{234}\mathrm{U} \rightarrow {}^{206}\mathrm{Hg} + {}^{28}\mathrm{Mg}$. One may expect that the formation of ^{26}Ne is more favored in ^{234}U (with the daughter system of ^{208}Pb). However, the decay emitting ^{26}Ne is hindered due to the presence of a much lower Q_c value (i.e., larger χ').

B. Systematics with the UDL

The prediction power of the UDL (Eq. (12)) on radioactive decay of medium and heavier nuclei has already been shown in our previous Letter [48]. Essentially, only the coefficients b and c are free parameters not provided by the UDL. Without loss of generalization, in that paper all coefficients of Eq. (12) are determined by fitting experimental data. The inclusion of a as a free parameter takes into account the effect of higher-order terms of the Coulomb penetrability. For example, the constants a, b and c corresponding to α-decay were determined to be 0.4065, -0.4311 and -20.7889, respectively [48]. The standard root mean square (rms) deviation between the UDL and experimental α-decay half-lives is $\sigma = 0.3436$. For the rms deviation we take the definition of Ref. [37],

$$\sigma = \left\{ \frac{1}{n-1} \sum_{i}^{n} \left[\log(T_i^{\mathrm{Cal.}}/T_i^{\mathrm{Expt.}}) \right]^2 \right\}^{1/2}, \tag{14}$$

where n is the number of decay events included in the fit and $T^{\mathrm{Expt.}}$ and $T^{\mathrm{Cal.}}$ the experimental and calculated decay half-lives, respectively. The fitted value for the coefficient a is close to the value calculated by its definition in Eqs. (9) and (12), namely $a = e^2\pi\sqrt{2m}/(\hbar \ln 10) = 0.4314$. Even if we fix the coefficient a at this value, the description power of the UDL is still encouraging, as illustrated in the upper plot of Fig. 4. With only two free parameters of b and c, the UDL can reproduce experimental α decay half-lives with a rms deviation of $\sigma = 0.4606$.

In some cases the experimental half-lives are noticeably underestimated by the UDL, with $T_{1/2}^{\mathrm{Expt.}}/T^{\mathrm{Cal.}} > 4$. These correspond to the α decays of ^{194,210}Pb, ^{208,210}Po and ^{212}Rn. This

TABLE I: Upper: Coefficient sets of Eq. (12) that determined by fitting to experiments of α decays (I), cluster decays (II) and both α and cluster decays (III), respectively [48], and the corresponding rms deviations; Lower: same as the upper part but with coefficient a fixed to its calculated value of $a = 0.4314$.

	I(α)	II(cluster)	III(α+cluster)
a	0.4065	0.3671	0.3949
b	-0.4311	-0.3296	-0.3693
c	-20.7889	-26.2681	-23.7615
σ	0.3436	0.6080	0.6107
a	0.4314	0.4314	0.4314
b	-0.4608	-0.3921	-0.4087
c	-21.9453	-32.7044	-25.7725
σ	0.4606	0.7901	0.7631

deviation may be related to the fact that the formation amplitudes in these nuclei, due to the shell closures of $N = 126$ and $Z = 82$, are significantly smaller than those in the open shell region.

In fig. 4 we plotted calculations with the UDL on α and heavier cluster decay half-lives and comparisons with experimental data. In these plots, the coefficient a of the UDL is taken as its calculated value while b and c are determined by fitting to corresponding experiments. In the figure we plotted the quantity $\log T_{1/2} - b\rho'$ as a function of χ'. Similar linear trend can be achieved if we plot experimental data as a function of ρ', as seen in Fig. 5 where all α and heavier cluster decays are considered. For all observed α and heavier cluster decays, the χ' and ρ' values are in the wide ranges of $105 < \chi' < 640$ and $60 < \rho' < 660$, respectively. As a result, the functions $\log T_{1/2} - b\rho'$ and $\log T_{1/2} - a\chi'$ we plotted in Figs. 4 and 5 change over 200 orders of magnitude. But the decay half-lives are in the range of $-8 < \log T_{1/2} < 28$ (in seconds).

In Table I the constants a, b and c that fit the data sets of α as well as cluster decays are collected. The fitted values with a as a free and fixed parameter are shown in the upper and lower part of the Table, respectively. In the table we also give the corresponding rms deviations between experiments and UDL calculations with these coefficient sets.

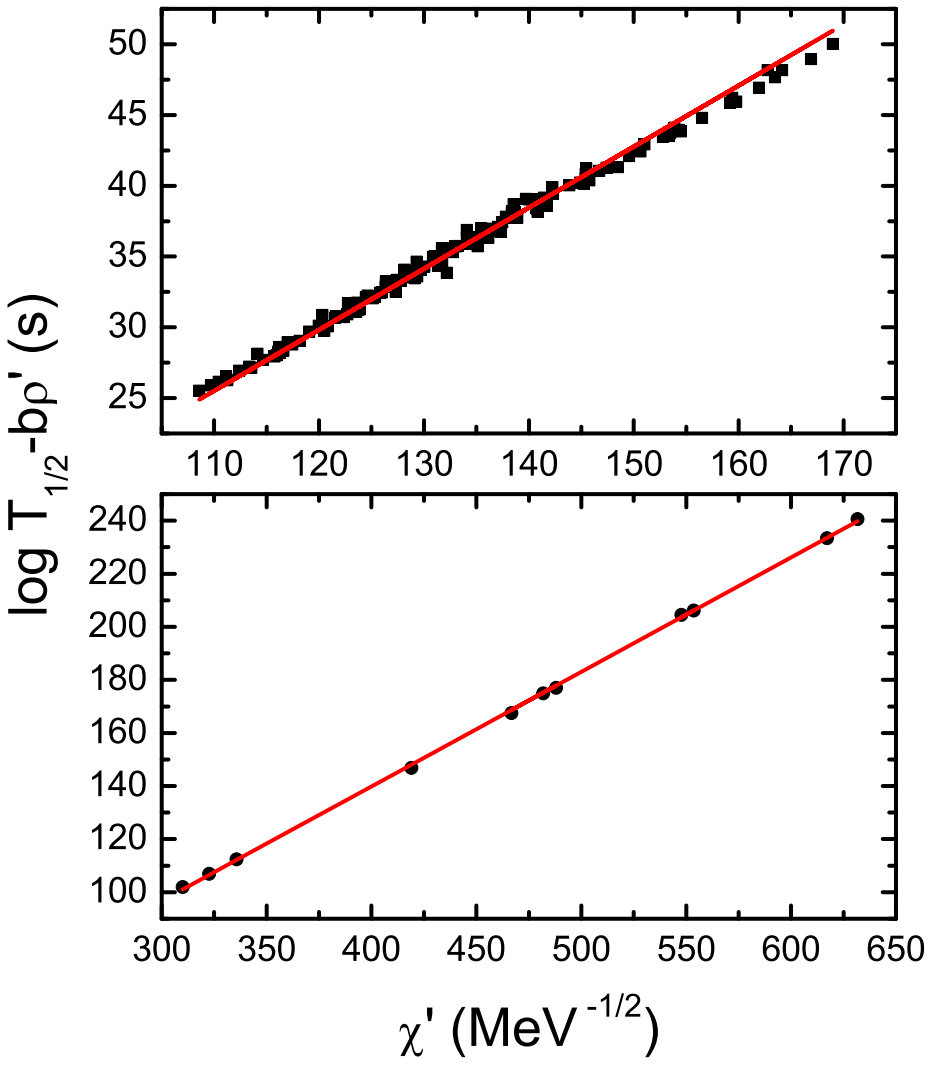

FIG. 4: (Color online) UDL description of α decays (upper panel) and heavier cluster decays (lower panel) with the coefficient a fixed at its calculated value. The black points correspond to experimental data with decay half-lives given in seconds. The lines are given as $a\chi' + c$ with c values from the lower part of Table I.

IV. PREDICTIONS AND DISCUSSIONS

Using the UDL it is straightforward to evaluate the half-lives of all cluster emitters throughout the nuclear chart if reliable values of the binding energies (i.e., of the cluster Q-values) can be obtained. We do this by using the latest compilation of nuclear masses [52].

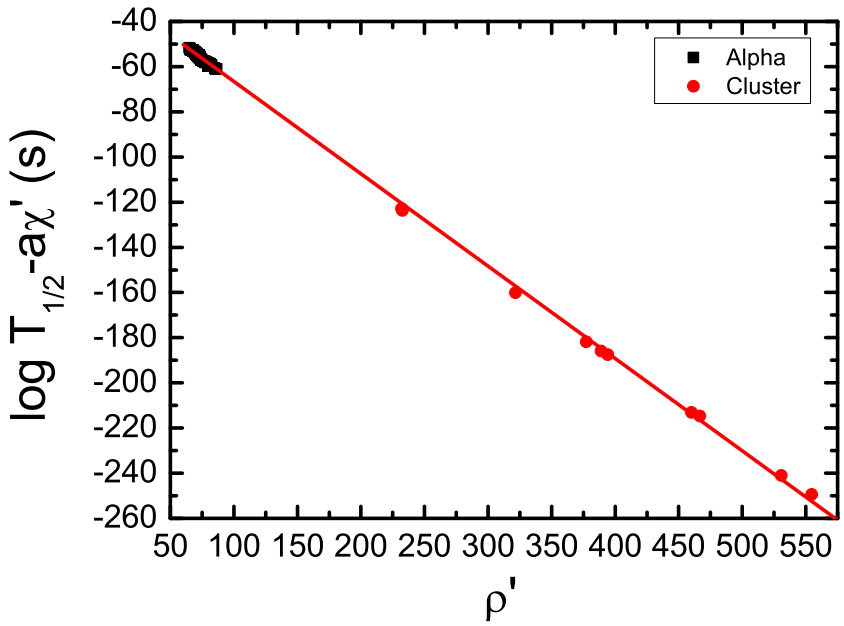

FIG. 5: (Color online) UDL description of both α and heavier cluster decays as a function of ρ'. The lines are given as $b\rho' + c$ with coefficients (set III) from the lower part of Table I.

With the Q-values thus obtained we evaluated the decay half-lives of all isotopes included in that compilation by applying the UDL. We will first show the case of the decay of α particles and afterwards that of other relevant clusters. For simplicity in what follows, only results calculated with coefficients from the upper part of Table I are shown.

Since the half-lives of decaying nuclei which live a very short or very large time can not be measured we will only consider even-even α emitters with half-lives in the 30 orders of magnitude range $-10 \leq \log T_{1/2} \leq 20$ (in second). The UDL predictions of the corresponding half-lives are shown in Fig. 6, employing the coefficient set I from the upper part of Table I. Within the constraints that we imposed a total number of 269 even-even α emitters have been found, which have charge numbers $Z \geq 52$. It is seen from the Figure that the most favored α decays are from neutron-deficient nuclei around the trans-lead and superheavy regions.

Since, as mentioned above, the emitters that we have used to determine the coefficients of the UDL (Table I) have charge number $Z \geq 78$, it would be interesting to probe the law for nuclei with Z-values below that limit. We thus took the extreme cases of decays from nuclei in the trans-tin region. The α decay properties of nuclei in this region has been intensively

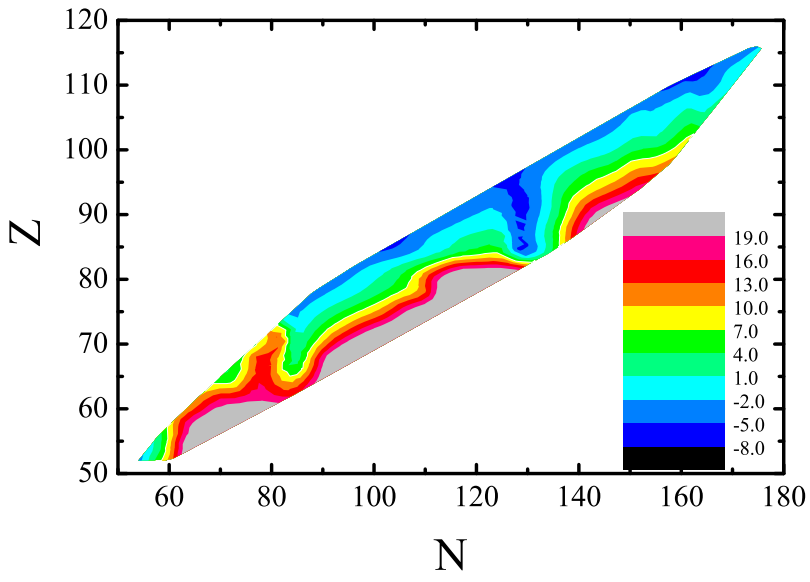

FIG. 6: (Color online) Prediction of the UDL (with the coefficient set I) on the logarithms of half-lives (in seconds), $\log T_{1/2}$, for the α decays of even-even nuclei.

TABLE II: Experimental and UDL calculated values (with the coefficient sets I and III) of α decay half-lives (in seconds) of even-even nuclei in the trans-tin region. Experimental data are taken from Ref. [1] except for the half-life of ^{110}Xe which is from Ref. [55].

Emitter	Q_α(MeV)	$\log T_{1/2}^{\rm Expt.}$	$\log T_{1/2}^{\rm Cal.}$(I)	$\log T_{1/2}^{\rm Cal.}$(III)
^{106}Te	4.290	-4.155	-3.446	-4.484
^{108}Te	3.445	0.6320	0.9761	-0.1812
^{110}Xe	3.885	-0.7850	-0.3774	-1.441
^{112}Xe	3.330	2.477	2.951	1.799
^{114}Ba	3.534	1.770	2.861	1.766

studied in recent years [55, 56, 57]. In Table II we compare experimental results on the α decays of Te, Xe and Ba isotopes and the predictions of the UDL. One sees that in all cases the experimental values lie between the ones calculated by using the parameters of the sets I and III in Table I, confirming the prediction power of the UDL.

We will now apply the UDL to evaluate the emissions of heavy clusters which are good candidates to be observed, namely ^{12,14}C, ^{16,18,20}O, ^{20,22,24}Ne, ^{24,26,28}Mg and ^{28,30,32,34}Si. Observed cluster radioactivities exhibit much longer partial half-lives than those of the corresponding α decays. This can be easily understood if we compare the χ' values of the heavier

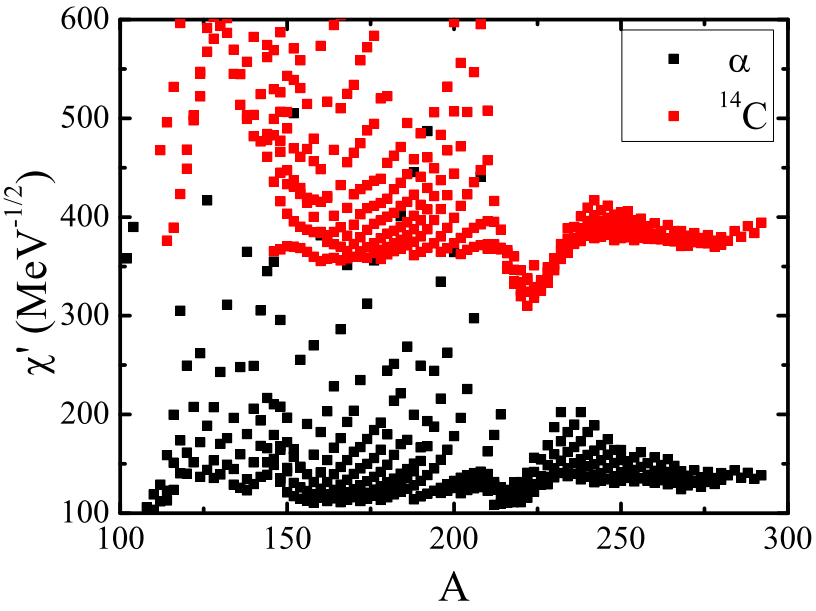

FIG. 7: (Color online) χ' values for α and ^{14}C radioactivities as a function of the mass numbers of mother nuclei.

cluster and α radioactivities since the logarithm of the half-life is proportional to χ'. As a typical example, in Fig. 7 we plotted the χ' values of α and ^{14}C decays as a function of the mass numbers of the mother nuclei. The χ' values of heavier clusters are mostly much higher than those of the corresponding α decays, indicating that it is more difficult for the heavier clusters to penetrate through the Coulomb barrier. Besides, from the figure one sees that nuclei favoring cluster decays should mostly be located in the trans-lead region.

In Fig. 8 we show the predicted half-lives corresponding to the most favored cluster radioactivity, namely ^{14}C decay. Our calculations show that nuclei like ^{220,222,224}Ra, ^{222,224}Th and ^{226}U can have partial decay half-lives shorter than 10^{16} s, among which the ^{14}C decays of ^{222,224}Ra have been observed [4, 7].

Our calculations also show that nuclei that most probably emit clusters with non-equal proton and neutron numbers like ^{14}C are concentrated in the trans-lead region. This is consistent with the expectation from the schematic picture of Fig. 7. For heavier clusters the formation probability is even smaller and therefore the corresponding decay probability is also smaller. As another typical example, in Fig. 9 we plotted calculations for the half-lives of the ^{24}Ne radioactivity. One sees in this Figure that the shortest half-lives correspond

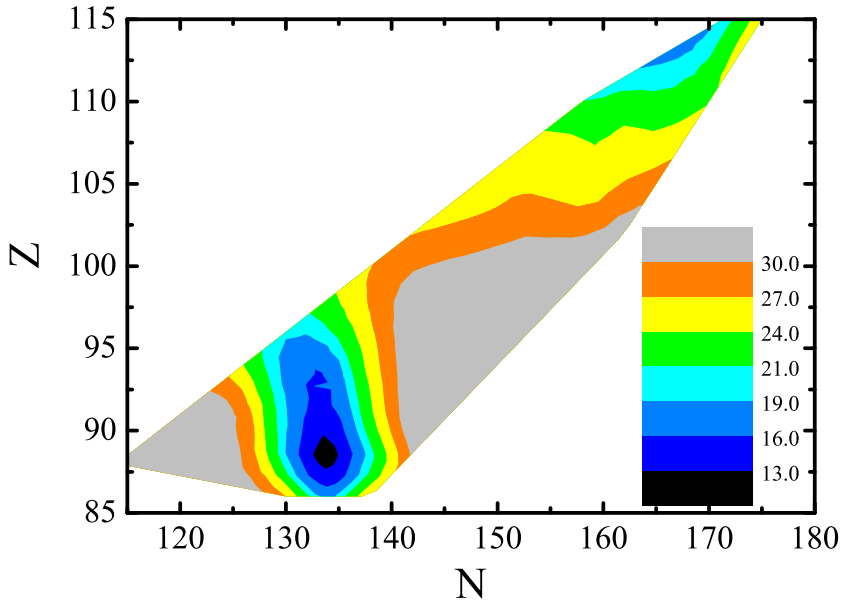

FIG. 8: (Color online) Same as Fig. 6 but for the ^{14}C cluster decay and with the coefficient set II.

to mother nuclei around Z=92 and N=138. In all cases this half-life is larger than 10^{21} s, which is many orders of magnitude larger than the cases corresponding to the decay of ^{14}C analyzed above.

All heavier-cluster-decaying nuclei decay also by emitting α particles. In fact α decay is usually the overwhelming dominant decay channel, as seen from Fig. 7. Therefore in planning the detection of a probable cluster decay one has to consider carefully the branching ratio of the α-decay channel relative to the corresponding cluster decay of interest, i.e., $b^{\rm rel.} = T^{\alpha}_{1/2}/T^{\rm cluster}_{1/2}$. The $\log b^{\rm rel}$ values are negative, which can not be too small for the heavier cluster decay to be detectable. We can evaluate these branching ratios by using the UDL. To search for probable cluster emitters we select particle decay channels for which neither the half-lives are too large nor the branching ratios are too small. We thus use the criteria $T_{1/2} < 10^{30}$ s and $b^{\rm rel.} > 10^{-18}$ which is two orders of magnitude outside present experimental limits. The corresponding calculations for the emissions of $N_c \neq Z_c$ clusters are listed in Table III. To give an insight of the expected precision, we present in Table IV comparisons between calculations and experiments for the half-lives of the eleven observed heavier cluster decay events of Fig. 4.

The α-decay mode dominates the decays of all heavier-cluster emitters we listed in Ta-

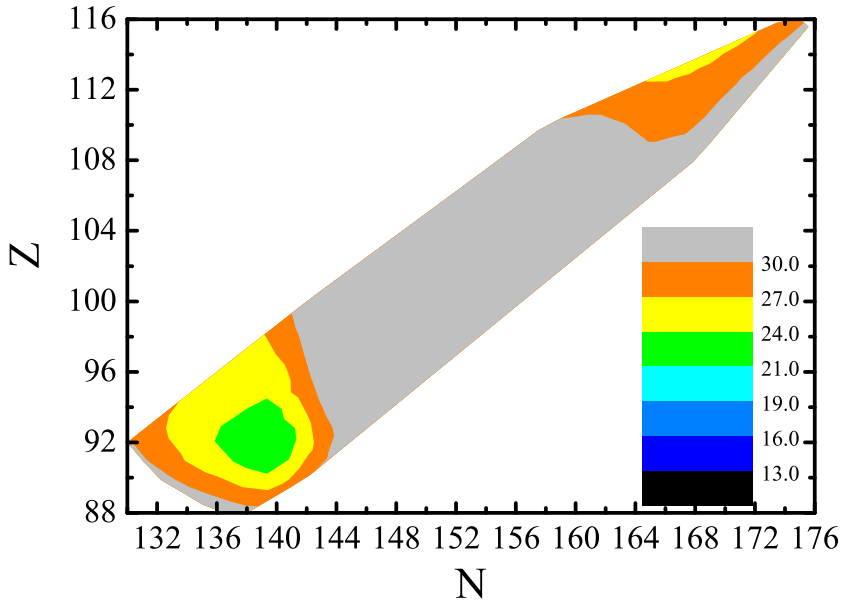

FIG. 9: (Color online) Same as Fig. 6 but for the ^{24}Ne decay.

ble III. In most cases the branching ratio between α decay and all other decay channels (including β decay) is $b^{\alpha} \simeq 100\%$ [1]. But there are exceptions, in particular the nuclei ^{232}Pu, ^{234}Pu and ^{238}Cm which have the α-decay branching ratios of $b^{\alpha} = 11\%$, $b^{\alpha} = 6\%$ and $b^{\alpha} < 10\%$, respectively [1].

We will now analyze the more rare case of radioactive decays of $N_c = Z_c$ clusters heavier than the α particle. Intense studies have been made in the prediction and searching for the emissions of $N_c = Z_c$ clusters [56, 57, 58, 59, 60, 61, 62]. Experiments have not pinned down the observation of these clusters yet, although efforts have been made, particularly looking for the probable emission of ^{12}C [60]. We have therefore apply the UDL to investigate regions in the nuclear chart where such cluster would be likely to be formed and emitted. The half-lives of ^{12}C decays thus calculated are plotted in Fig. 10. The emissions of other $N_c = Z_c$ clusters like ^{16}O show similar patterns. It is seen from the figure that $N_c = Z_c$ cluster emitters form two islands, decaying into daughter nuclei around ^{100}Sn and ^{208}Pb. This is consistent with theoretical calculations using the fission model [8, 61].

A first glance at Fig. 10 may suggest that the emissions of $N_c = Z_c$ clusters like ^{12}C should be more favored than those of other $N_c \neq Z_c$ isotopes since the former particle is usually more tightly bound. Such a picture is also expected if we compare the χ' values for

TABLE III: Predictions of the UDL on probable emissions of $N_c \neq Z_c$ clusters.

Emitter	Mode	Q_c(MeV)	$\log T_{1/2}^{\rm cluster}$ (s)	$-\log b^{\rm rel.}$
^{220}Rn	^{14}C	28.539	17.759	15.573
^{222}Rn	^{14}C	26.451	22.313	16.399
^{220}Ra	^{14}C	31.038	14.776	16.142
^{222}Th	^{14}C	31.653	15.466	17.776
^{224}Th	^{14}C	32.930	13.057	12.657
^{226}Th	^{14}C	30.547	17.454	13.747
^{228}Th	^{14}C	28.222	22.278	14.082
^{230}Th	^{14}C	26.060	27.340	14.605
^{226}U	^{14}C	32.969	14.774	14.993
^{228}U	^{14}C	30.525	19.394	16.308
^{230}U	^{14}C	28.339	24.025	17.331
^{228}Pu	^{14}C	32.968	16.572	16.858
^{226}Th	^{18}O	45.727	18.235	14.529
^{228}Th	^{18}O	42.282	23.933	15.737
^{230}Th	^{18}O	39.193	29.674	16.938
^{228}U	^{18}O	45.959	20.083	16.996
^{226}Ra	^{20}O	40.817	26.217	15.189
^{230}Th	^{20}O	41.795	26.762	14.026
^{232}U	^{22}Ne	57.364	26.532	16.784
^{232}Pu	^{22}Ne	62.343	21.941	17.671
^{228}Th	^{24}Ne	57.414	25.393	17.197
^{232}Th	^{24}Ne	54.497	29.916	11.951
^{230}U	^{24}Ne	61.352	22.171	15.477
^{234}U	^{24}Ne	58.826	25.727	12.542
^{234}Pu	^{24}Ne	62.254	23.382	17.336
^{232}U	^{26}Mg	71.771	27.481	17.732
^{232}Pu	^{26}Mg	78.366	21.852	17.583
^{234}Pu	^{26}Mg	78.313	21.786	15.739
^{232}U	^{28}Mg	74.320	25.201	15.453
^{234}Pu	^{28}Mg	79.154	21.807	15.760
^{238}Pu	^{28}Mg	75.912	25.800	16.154
^{238}Cm	^{28}Mg	80.368	23.023	17.547
^{238}Cm	^{30}Si	95.577	22.601	17.125
^{236}Pu	^{32}Si	91.674	24.941	16.741
^{238}Cm	^{32}Si	97.262	21.513	16.037
^{240}Cm	^{32}Si	97.555	21.020	14.559
^{238}Pu	^{34}Si	90.812	26.753	17.106
^{240}Pu	^{34}Si	91.029	26.322	14.728
^{240}Cm	^{34}Si	95.468	24.290	17.829

the radioactive decays of other isotopes. A typical example is given in Fig. 11 where we plotted the χ' values of the ^{12}C and ^{14}C radioactivities. It is seen that the χ' values of the ^{12}C radioactivity are mostly smaller that those of ^{14}C, indicating that it should be much easier for the ^{12}C particle to penetrate through the Coulomb barrier, especially in nuclei close to the proton drip line. However, the probability of the decay of $N_c = Z_c$ clusters

TABLE IV: Experimental and UDL calculated values (with the coefficient set II of cluster decay half-lives (in seconds). The experimental values are from Ref. [7].

Emitter	Mode	Q_c(MeV)	$\log T_{1/2}^{\rm Expt.}$	$\log T_{1/2}$(II)
^{222}Ra	^{14}C	33.05	11.01	11.07
^{224}Ra	^{14}C	30.54	15.86	15.59
^{226}Ra	^{14}C	28.20	21.24	20.33
^{228}Th	^{20}O	44.72	20.72	21.59
^{230}U	^{22}Ne	61.39	19.22	20.73
^{230}Th	^{24}Ne	57.76	24.61	24.74
^{232}U	^{24}Ne	62.31	20.40	20.68
^{234}U	^{28}Mg	74.11	25.75	25.36
^{236}Pu	^{28}Mg	79.67	21.52	21.02
^{238}Pu	^{32}Si	91.19	25.27	25.39
^{242}Cm	^{34}Si	96.51	23.15	22.87

become small if we take into account the fact that the likely emitters are mostly close to the proton drip line and are dominated by the decay mode of β^+. With the same selection criteria discussed above, our predictions on probable emissions of $N_c = Z_c$ clusters are listed in Table V. Since in all cases the decay by the emission of an α particle is much more likely than the corresponding decay by the emission of heavier clusters, in Table V we only show emitters that are known to decay α [1]. It is seen from the Table that the mostly likely $N_c = Z_c$ cluster emitter is the nucleus ^{114}Ba.

V. SUMMARY AND CONCLUSIONS

Starting from the exact expression for the half-life of cluster decaying nuclei (Eq. (2)) we found that this expression is dependent upon a quantity called $\cos^2\beta$ which for medium and heavier nuclei is small (Eq. (4)). For the case of $l = 0$ (monopole) transitions we expanded the exact expression to the lowest order in $\cos^2\beta$ and used the property that the half-life does not depend upon the matching radius R (Eq. (11)). We thus found that the logarithm of the half-life is linearly dependent upon two parameters, called χ' and ρ', which depend only upon the Q-value of the outgoing cluster and of the charges and masses of the particles involved in the decay (Eq. (8)). The resulting linear expression (Eq. (12)) is found to be a generalization of the Geiger-Nuttall law and we call it the universal decay law (UDL). The UDL is valid for all $l = 0$ transitions. This monopole linear equation contains three constants, called a, b and c. We fitted the experimental half-lives of ground-state to ground-

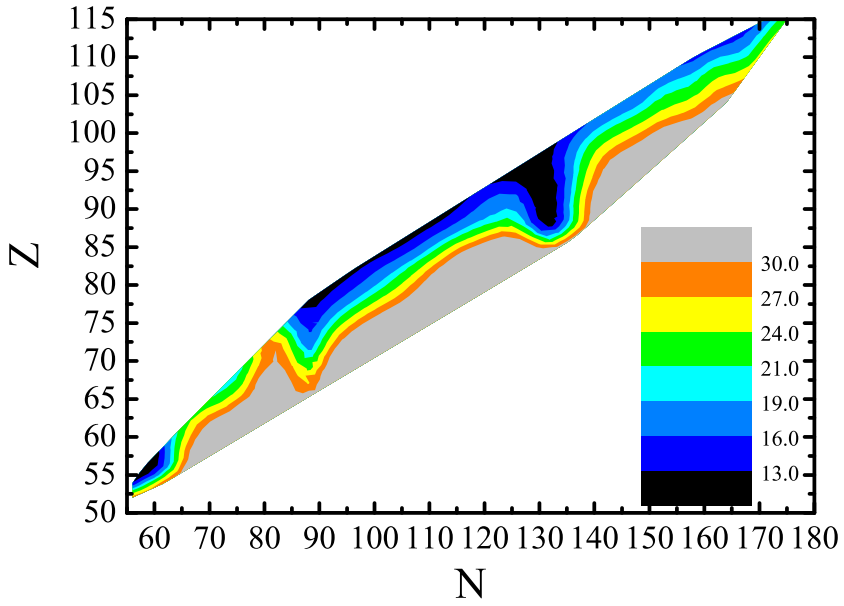

FIG. 10: (Color online) Same as Fig. 6 but for the ^{12}C decay.

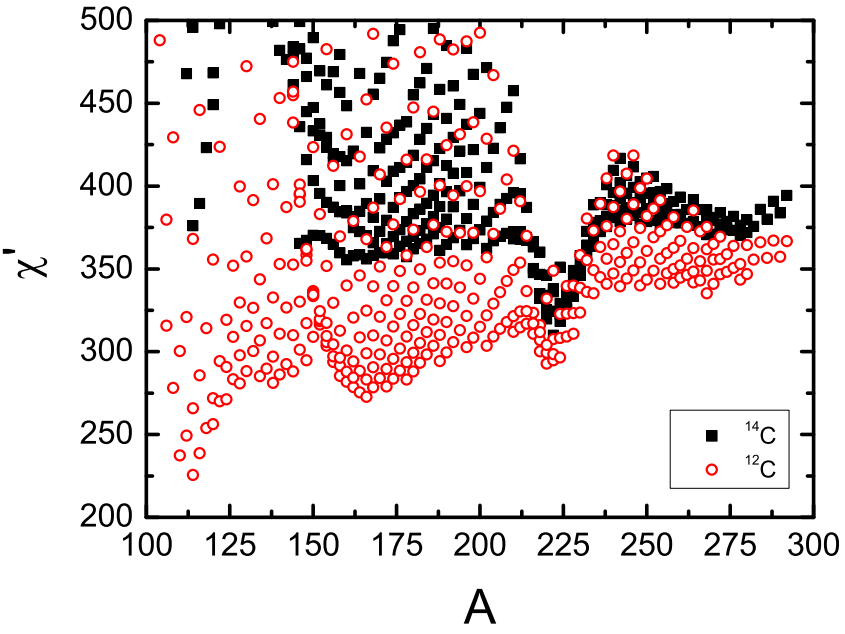

FIG. 11: (Color online) χ' values for ^{12}C and ^{14}C radioactivities as a function of the mass numbers of mother nuclei.

TABLE V: Predictions of the UDL on probable emissions of $N_c = Z_c$ clusters. The α decay branching ratios, b^α, of the cluster emitters are taken from Ref. [1].

Emitter	Mode	Q_c(MeV)	$\log T_{1/2}^{\rm cluster}$(s)	$-\log b^{\rm rel.}$	b^α(%)
^{110}Xe	^{12}C	15.726	12.863	13.241	64
^{112}Xe	^{12}C	14.283	17.099	14.148	0.9
^{114}Ba	^{12}C	18.984	7.199	4.338	0.9
^{154}Dy	^{12}C	15.557	28.193	14.432	100
^{158}Yb	^{12}C	20.078	19.374	12.888	2.1E-3
^{160}Hf	^{12}C	21.922	17.015	13.640	0.7
^{162}Hf	^{12}C	20.144	21.415	15.362	8E-3
^{162}W	^{12}C	23.831	14.813	14.100	45.2
^{166}W	^{12}C	20.720	22.080	17.505	3.5E-2
^{166}Os	^{12}C	24.495	15.339	15.644	72
^{168}Os	^{12}C	23.274	17.959	17.000	49
^{166}Pt	^{12}C	27.941	10.616	14.039	100
^{168}Pt	^{12}C	26.815	12.619	15.159	100
^{170}Pt	^{12}C	25.799	14.537	16.133	8.6
^{172}Pt	^{12}C	24.836	16.463	17.222	72
^{172}Hg	^{12}C	28.275	11.680	15.146	100
^{174}Hg	^{12}C	27.355	13.311	15.905	100
^{176}Hg	^{12}C	26.454	14.993	16.504	90
^{180}Hg	^{12}C	24.645	18.666	17.879	48
^{178}Pb	^{12}C	29.006	12.013	15.597	100
^{180}Pb	^{12}C	28.052	13.691	16.164	100
^{184}Pb	^{12}C	26.193	17.231	17.600	80
^{202}Ra	^{12}C	29.630	15.569	17.955	100
^{218}Ra	^{12}C	30.436	13.497	17.715	100
^{220}Ra	^{12}C	32.021	10.662	12.027	100
^{222}Ra	^{12}C	29.049	15.957	14.029	100
^{224}Ra	^{12}C	26.375	21.476	15.609	100
^{226}Ra	^{12}C	23.850	27.524	16.496	100
^{220}Th	^{12}C	32.139	12.227	16.852	100
^{222}Th	^{12}C	33.156	10.455	12.765	100
^{224}Th	^{12}C	30.366	15.248	14.848	100
^{226}Th	^{12}C	27.667	20.569	16.863	100
^{222}U	^{12}C	33.897	10.968	16.320	100
^{224}U	^{12}C	34.373	10.132	13.178	100
^{226}U	^{12}C	31.649	14.651	14.869	100
^{228}U	^{12}C	28.969	19.714	16.627	> 95
^{228}Pu	^{12}C	32.797	14.327	14.613	100
^{112}Xe	^{16}O	21.000	20.519	17.568	0.9
^{114}Ba	^{16}O	26.422	11.477	8.616	0.9
^{162}Hf	^{16}O	31.657	21.563	15.510	8E-3
^{166}Os	^{16}O	37.132	16.535	16.839	72
^{168}Pt	^{16}O	40.005	14.214	16.754	100
^{172}Hg	^{16}O	41.502	14.053	17.518	100
^{224}Th	^{16}O	46.482	15.321	14.921	100
^{226}Th	^{16}O	42.662	21.196	17.489	100
^{226}U	^{16}O	48.019	15.152	15.371	100
^{228}U	^{16}O	44.331	20.657	17.570	> 95
^{228}Pu	^{16}O	49.485	15.095	15.381	100

state α-decay and heavier cluster decay processes in even-even nuclei to obtain the values of the constants given in Table I. We found that the UDL predicts with great precision the half-lives of radioactive decays, both α- and cluster-decays, and for all isotopic series, as expected since the original exact expression for the half-life is valid in general. This law may also help in the ongoing search of new cluster decay modes from superheavy nuclei.

Using the UDL we have evaluated the decay half-lives of various cluster emitters throughout the nuclear chart with reliable values of binding energies as input. It is found that the α decay is favored in neutron-deficient nuclei around the trans-lead and superheavy regions. The decays of heavier clusters with non-equal proton and neutron numbers are mostly located in the trans-lead region. The probability of the decay of clusters with equal numbers of protons and neutrons is small since the likely emitters are mostly close to the proton drip line and are dominated by the decay mode of β^+.

An important conclusion from the UDL is that the cluster formation amplitude $F_c(R)$ is exponentially dependent upon the variable ρ'. The implication of this linear trend on nuclear structure effects may deserve further investigations in the future.

Acknowledgments

This work has been supported by the Chinese Major State Basic Research Development Program under Grant 2007CB815000; the National Natural Science Foundation of China under Grant Nos. 10525520, 10735010 and 10875172 and the Swedish Science Research Council (VR).

---

[1] G. Audi, O. Bersillon, J. Blachol, and A.H. Wapstra, Nucl. Phys. A **729**, 3 (2003).

[2] A.A. Sonzogni, Nucl. Data Sheets **95**, 1 (2002).

[3] A. Sandulescu, D.N. Poenaru, and W. Greiner, Sov. J. Part. Nucl. **11**, 528 (1980).

[4] H.J. Rose and G.A. Jones, Nature (London) **307**, 245 (1984).

[5] P.B. Price, Annu. Rev. Nucl. Part. Sci. **39**, 19 (1989).

[6] E. Hourani, M. Hussonnois, and D.N. Poenaru, Ann. Phys. (Paris) **14**, 311 (1989).

[7] R. Bonetti and A. Guglielmetti, Roman. Rep. Phys. **59**, 301 (2007).

[8] W. Greiner, M. Ivascu, D.N. Poenaru, S. Sandulescu, in Treatise on Heavy Ion Science, edited by D.A. Bromley (Plenum, New York, 1989), Vol.8, p.641.

[9] D.N. Poenaru, D. Schnabel, W. Greiner, D. Mazilu, and R. Gherghescu, At. Data Nucl. Data Tables **48**, 231 (1991).

[10] Y.J. Shi and W.J. Swiatecki, Phys. Rev. Lett. **54**, 300 (1985).

[11] O. Dumitrescu, Phys. Rev. C **49**, 1466 (1994).

[12] B. Buck and A.C. Merchant, J. Phys. G: Nucl. Part. Phys. **15**, 615 (1989).

[13] B. Buck, A.C. Merchant, S.M. Perez, At. Dat. Nucl. Dat. Tables **54**, 53 (1993).

[14] R. Blendowske and H. Walliser, Phys. Rev. Lett. **61**, 1930 (1988).

[15] D.S. Delion, A. Insolia, and R.J. Liotta, J. Phys. G: Nucl. Part. Phys. **20**, 1483 (1994); Phys. Rev. Lett. **78**, 4549 (1997).

[16] R.G. Lovas, R.J. Liotta, A. Insolia, K. Varga, and D.S. Delion, Phys. Rep. **294**, 265 (1998).

[17] H.J. Mang, Annu. Rev. Nucl. Sci. **14**, 1 (1964).

[18] A. Arima and S. Yoshida, Nucl. Phys. **A219**, 475 (1974).

[19] D.S. Delion, R.J. Liotta, and R. Wyss, Phys. Rep. **424**, 113 (2006).

[20] M. Bhattacharya and G. Gangopadhyay, Phys. Rev. C **77**, 027603 (2008).

[21] F.R. Xu and J.C. Pei, Phys. Lett. **B 642**, 322 (2006).

[22] H.F. Zhang and G. Royer, Phys. Rev. C **77**, 054318 (2008).

[23] T.R. Routray, J. Nayak, D.N. Basu, Nucl. Phys. A **826**, 223 (2009).

[24] A. Bhagwat and Y.K. Gambhir, J. Phys. G: Nucl. Part. Phys. **35**, 065109 (2008).

[25] D. Ni, Z. Ren, Phys. Rev. C **80**, 014314 (2009).

[26] R.G. Thomas, Prog. Theor. Phys. **12**, 253 (1954).

[27] G. Gamow, Z. Phys. **51**, 204 (1928); Z. Phys. **52**, 510 (1929).

[28] M. Iriondo, D. Jerrestam, and R.J. Liotta, Nucl. Phys. A**454**, 252 (1986).

[29] D.N. Poenaru, Y. Nagame, R.A. Gherghescu, and W. Greiner, Phys. Rev. C **65**, 054308 (2002).

[30] R. Blendowske, T. Fliessbach, and H. Walliser, Z. Phys. A **339**, 121 (1991).

[31] H. Geiger and J.M. Nuttall, Philos. Mag. **22**, 613 (1911); H. Geiger, Z. Phys. **8**, 45 (1922).

[32] B. Buck, A.C. Merchant, and S.M. Perez, Phys. Rev. Lett.**65**, 2975 (1990).

[33] V.E. Viola and G.T. Seaborg, J. Inorg. Nucl. Chem. **28**, 741 (1966).

[34] B.A. Brown, Phys. Rev. C **46**, 811 (1992).

[35] P. Möller, J.R. Nix, and K.-L. Kratz, Atom. Data and Nucl. Data Tables **66**, 131 (1997).

[36] G. Royer, J. Phys. G: Nucl. Part. Phys. **26**, 1149 (2000).

[37] D.N. Poenaru, I.H. Plonski, and W. Greiner, Phys. Rev. C **74**, 014312 (2006).

[38] V. Yu. Denisov and A.A. Khudenko, Phys. Rev. C **79**, 054614 (2009).

[39] D.S. Delion, R.J. Liotta, and R. Wyss, Phys. Rev. Lett. **96**, 072501 (2006).

[40] E.L. Medeiros, M.M.N. Rodrigues, S.B. Duarte and O.A.P. Tavares, Eur. J. Phys. A **34**, 417 (2007).

[41] J.M. Dong, H.F. Zhang, and G. Royer, Phys. Rev. C **79**, 054330 (2009).

[42] Z. Ren, C. Xu, and Z. Wang, Phys. Rev. C **70**, 034304 (2004).

[43] M. Balasubramaniam, S. Kumarasamy, N. Arunachalam, and Raj K. Gupta, Phys. Rev. C **70**, 017301 (2004).

[44] M. Horoi, J. Phys. G: Nucl. Part. Phys. **30**, 945 (2004).

[45] D. Ni, Z. Ren, T. Dong, and C. Xu, Phys. Rev. C **78**, 044310 (2008).

[46] K.P. Santhosh, R.K. Biju, and A. Joseph, J. Phys. G: Nucl. Part. Phys. **35**, 085102 (2008).

[47] D.S. Delion, Phys. Rev. C **80**, 024310 (2009); arXiv: 0907.2304.

[48] C. Qi, F.R. Xu, R.J. Liotta, and R. Wyss, Phys. Rev. Lett. **103**, 072501 (2009).

[49] A.M. Lane and R.G. Thomas, Rev. Mod. Phys. **30**, 257 (1958).

[50] E. Maglione, L.S. Ferreira, and R.J. Liotta, Phys. Rev. Lett. **81**, 538 (1998).

[51] P.O. Fröman, Mat. Fys. Skr. Dan. Vidensk. Selsk. **1**, no. 3 (1957).

[52] G. Audi, A.H. Wapstra, and C. Thibault, Nucl. Phys. A **729**, 337 (2003).

[53] J.C. Pei, F.R. Xu, Z.J. Lin, and E.G. Zhao, Phys. Rev. C **76**, 044326 (2007).

[54] J. Dvorak *et al.*, Phys. Rev. Lett. **97**, 242501 (2006).

[55] Z. Janas *et al.*, Eur. Phys. J. A **23**, 197 (2005).

[56] C. Mazzocchi *et al.*, Phys. Lett. B **532**, 29 (2002).

[57] I. Silisteanu, W. Scheid, and A. Sandulescu, Nucl. Phys. A **679**, 317 (2001).

[58] Yu. Ts. Oganessian *et al.*, Z. Phys. A **349**, 341 (1994).

[59] A. Guglielmetti *et al.*, Phys. Rev. C **52**, 740 (1995).

[60] A. Guglielmetti *et al.*, Phys. Rev. C **56**, R2912 (1997).

[61] D.N. Poenaru, W. Greiner, and R. Gherghescu, Phys. Rev. C **47**, 2030 (1993).

[62] S. Kumar, D. Bir, and R.K. Gupta, Phys. Rev. C **51**, 1762 (1995).